Site-Directed Mutagenesis of Active Site Residues of Phosphite Dehydrogenase†

Ryan Woodyer, Joshua L. Wheatley, Heather A. Relyea, Stacey Rimkus, and Wilfred A. van der Donk*

Department of Chemistry, University of Illinois at Urbana-Champaign, 600 South Mathews Avenue, Urbana, Illinois 61801

Received October 2, 2004; Revised Manuscript Received December 27, 2004

ABSTRACT: Phosphite dehydrogenase (PTDH) catalyzes the unusual oxidation of phosphite to phosphate with the concomitant reduction of NAD^+ to NADH. PTDH shares significant amino acid sequence similarity with D-hydroxy acid dehydrogenases (DHs), including strongly conserved catalytic residues His292, Glu266, and Arg237. Site-directed mutagenesis studies corroborate the essential role of His292 as all mutants of this residue were completely inactive. Histidine-selective inactivation studies with diethyl pyrocarbonate provide further evidence regarding the importance of His292. This residue is most likely the active site base that deprotonates the water nucleophile. Kinetic analysis of mutants in which Arg237 was changed to Leu, Lys, His, and Gln revealed that Arg237 is involved in substrate binding. These results agree with the typical role of this residue in D-hydroxy acid DHs. However, Glu266 does not play the typical role of increasing the pK_a of His292 to enhance substrate binding and catalysis as the Glu266Gln mutant displayed an increased k_{cat} and unchanged pH−rate profile compared to those of wild-type PTDH. The role of Glu266 is likely the positioning of His292 and Arg237 with which it forms hydrogen bonds in a homology model. Homology modeling suggests that Lys76 may also be involved in substrate binding, and this postulate is supported by mutagenesis studies. All mutants of Lys76 display reduced activity with large effects on the K_m for phosphite, and Lys76Cys could be chemically rescued by alkylation with 2-bromoethylamine. Whereas a positively charged residue is absolutely essential for activity at the position of Arg237, Lys76 mutants that lacked a positively charged side chain still had activity, indicating that it is less important for binding and catalysis. These results highlight the versatility of nature's catalytic scaffolds, as a common framework with modest changes allows PTDH to catalyze its unusual nucleophilic displacement reaction and D-hydroxy acid DHs to oxidize alcohols to ketones.

Phosphorus-containing molecules play essential roles in all organisms. Most of these compounds involve phosphorus in its +5 oxidation state such as the ubiquitous phosphate esters (RNA and DNA) and anhydrides (NTPs[1] and NDPs). As a result, studies on enzymes involved in phosphorus metabolism have been largely confined to phosphate ester/anhydride formation and hydrolysis. Essentially unexplored, with a few notable exceptions of enzymes that catalyze formation and cleavage of the C−P bond (*1*−*5*), are transformations that involve changes in the phosphorus oxidation state. Phosphite dehydrogenase (PTDH) catalyzes the NAD^+-dependent oxidation of hydrogen phosphonate (phosphite) to phosphate (*6*). PTDH and the recently reported hypophosphite dioxygenase (*7*) are the only known enzymes that catalyze direct oxidation of compounds containing a reduced phosphorus atom. PTDH has practical value as an NAD(P)H cofactor regeneration enzyme in biotechnology and may be useful for the preparation of isotopically labeled products or nonproteinogenic amino acids (*8*−*10*).

The amino acid sequence of PTDH from *Pseudomonas stutzeri* WM88 (*6*) is significantly homologous (23−34% identity) with the sequence of the family of D-isomer specific 2-hydroxyacid dehydrogenases (DHs, Figure 1) (*11*). The chemistry catalyzed by PTDH is, however, fundamentally different from that promoted by the other family members as it involves nucleophilic displacement of one of the phosphorus ligands (hydride) rather than a change in hybridization (Scheme 1). The closest similarity with the reaction catalyzed by PTDH may be the oxidation of the hydrated form of glyoxylate to oxalate by L-lactate DH (*12*−*15*), but PTDH does not show any activity with hydrated aldehyde substrates (*16*). In essence, the transformation catalyzed by PTDH is formally a phosphoryl transfer reaction. While hydride would normally be an exceptionally poor leaving group for nucleophilic displacement, a strong driving force for the reaction is provided by the very favorable thermodynamics of oxidizing phosphite to phosphate ($E^{\circ\prime} = -0.648$ V at pH 7) and reducing NAD^+ to NADH ($E^{\circ\prime} = -0.320$ V), a process that is overall ∼15 kcal/mol exergonic. Despite the favorable energetics, no other members of the D-hydroxy acid DH family tested so far have displayed any phosphite oxidation activity (*16*). The strong exergonic nature of the reaction notwithstanding, the hydride

† Support for this research was provided by the National Institutes of Health (Grant GM 63003). S.R. is a Colgate-Palmolive Undergraduate Fellow.

* To whom correspondence should be addressed. Phone: (217) 244-5360. Fax: (217) 244-8024. E-mail: vddonk@uiuc.edu.

[1] Abbreviations: DH, dehydrogenase; DEPC, diethyl pyrocarbonate; DGDH, D-glycerate dehydrogenase; DLDH, D-lactate dehydrogenase; DPGDH, D-3-phosphoglycerate dehydrogenase; FPLC, fast protein liquid chromatography; FDH, formate dehydrogenase; HPLC, high-performance liquid chromatography; IMAC, immobilized metal affinity chromatography; IPTG, isopropyl β-D-thiogalactopyranoside; NAD^+ and NADH, nicotinamide adenine dinucleotide; NDPs, nucleoside diphosphates; NTPs, nucleoside triphosphates; Pt, phosphite; PTDH, phosphite dehydrogenase; PCR, polymerase chain reaction; wt, wild-type.

10.1021/bi047868c CCC: $30.25
Published on Web 03/05/2005

```
PTDH            LQLLAPHCELMTNQTDSTLTREEILRRCRDAQAMM--AFMPDRVDADFLQACPE--LRVV 71
NP_478512       IELLKPSCEVIANPSKEALSREEILQRAKDAEALM--VFMPDTIDEAFLRECPK--LKII 71
ZP_00110436     ITNLSEYCEVVANPTRETLPREEILKLAQDAEALM--VFMPDRIDEAFLKACPK--LKII 71
DGDH            MARARESYDVIAHGDDPKITIDEMIETAKSVDALL--ITLNEKCRKEVIDRIPEN-IKCI 73
PGDH            LESLRAAGYTNIEFHKGALDDEQLKESIRDAHFIG--LRSRTHLTEDVINAAEK--LVAI 79
DLDH            LNEWKEAHKDIDVDYTDKLLTPETAKLAKGADGVV--VYQQLDYTADTLQALADAGVTKM 74
FDH             RKYLESNGHTLVVTSDKDGPDSVFERELVDADVVISQPFWPAYLTPERIAKAKN--LKLA 118

PTDH            GCALKGFDNFDVDACTARGVWLTFVPDLLTVPTAELAIGLAVGLGRHLRAADAFVRSGEF 131
NP_478512       AAALKGYDNFDVAACTHRGIWFTIVPSLLSAPTAEITIGLLIGLGRQMLEGDRFIRTGKF 131
ZP_00110436     AGALKGYDNFDVDACTRQGIWFTIVPSLLAVPTAELTIGLIIGLARQMLLGDRLIRQGTF 131
DGDH            STYSIGFDHIDLDACKARGIKVGNAPHGVTVATAEIAMLLLLGSARRAGEGEKMIRTRSW 133
PGDH            GCFCIGTNQVDLDAAAKRGIPVFNAPFSNTRSVAELVIGELLLLLRGVPEANAKAHRGVW 139
DLDH            SLRNVGVDNIDMDKAKELGFQITNVPVYSPNAIAEHAAIQAARVLRQDKRMDEKMAKRDL 134
FDH             LTAGIGSDHVDLQSAIDRNVTVAEVTYCNSISVAEHVVMMILSLVRNYLPSHEWARKGGW 178
                     G    D                        AE          R

PTDH            QGWQP-QFYGTGLDNATVGILGMGAIGLAMADRLQGWGATLQYHEAKALDTQTEQRLGLR 190
NP_478512       TGWRP-QFYSLGLANRTLGIVGMGALGKAIAGRLAGFEMQLLYSDPVALPPEQEATGNIS 190
ZP_00110436     AGWRP-HLYGMGLANRTLGIVGMGSLGQALAQRLSSFEMNLIYTDAIPLPKEKAAAWCLS 190
DGDH            PGWEPLELVGEKLDNKTLGIYGFGSIGQALAKRAQGFDMDIDYFDTHRASSSDEASYQAT 193
PGDH            NKLAAGSFEAR---GKKLGIIGYGHIGTQLGILAESLGMYVYFYDIENKLPLGNATQVQH 196
DLDH            R-WAP--TIGREVRDQVVGVVGTGHIGQVFMRIMEGFGAKVIAYDIFKNPELEKKGYYVD 191
FDH             N-IADCVSHAYDLEAMHVGTVAAGRIGLAVLRRLAPFDVHLHYTDRHRLPESVEKELNLT 237
                               G  g G  G                d

PTDH            -QVACSELFASSDFILLALPLNADTQHLVNAELLALVRPGALLVNPCRGSVVDEAAVLAA 249
NP_478512       -RVPFETLIESSDFVVLVVPLQPATLHLINANTLAKMKPGSFLINPCRGSVVDEQAVCKA 249
ZP_00110436     -QVSLDTLLATSDFVVLMVPLQPETFHLINEKSLARMKPGSFLINPCRGSVVDEQAVSDA 249
DGDH            FHDSLDSLLSVSQFFSLNAPSTPETRYFFNKATIKSLPQGAIVVNTARGDLVDNELVVAA 253
PGDH            ----LSDLLNMSDVVSLHVPENPSTKNMMGAKEISLMKPGSLLINASRGTVVDIPALCDA 252
DLDH            ---SLDDLYKQADVISLHVPDVPANVHMINDKSIAEMKDGVVIVNCSRGRLVDTDAVIRG 248
FDH             WHATREDMYPVCDVVTLNCPLHPETEHMINDETLKLFKRGAYIVNTARGKLCDRDAVARA 297
                              L  P                  G    N  RG   D      .

PTDH            LERGQLGGYAADVFEMEDWARADRPRLIDPALLAHPN-TLFTPHIGSAVRAVRL 302
NP_478512       LESGHLAGYAADVFEMEDWYRSDRPHNIPQPLLENTKQTFFTPHIGSAVDELRH 303
ZP_00110436     LASGHLAGYAADVFELEDWARSDRPSKIPPSLLEKQDQTFFTPHLGSAVDDLRY 303
DGDH            LEAGRLAYAGFDVFAGEPNINEGYYDLPN-TFLFPHIGSAATQARE 298
PGDH            LASKHLAGAAIDVFPTEPATNSDPFTSPLCEFDN-VLLTPHIGGSTQEAQE 302
DLDH            LDSGKIFGFVMDTYEDEVGVFNKDWEGKEFPDKRLADLIDRPN-VLVTPHTAFYTTHAVR 307
FDH             LESGRLAGYAGDVWFPQPAPKDHPWRTMPYNG---MTPHISGTTLTAQA 343
                L          D    e                          PH
```

FIGURE 1: Partial sequence alignment of PTDH with members of the D-hydroxy acid dehydrogenase family. Conserved residues are indicated in the consensus sequence. In blue are residues of the signature fingerprint motif ($GX_2GXGX_2GX_{17}D$) for a Rossmann fold for binding the cofactor (*51*, *52*), except that in PTDH the usual Asp is replaced with Glu. In yellow are three residues, Arg237, Glu266, and His292 (PTDH numbering), that have important catalytic functions in the hydroxyacid dehydrogenases (*20*−*22*). The Gly and Val/Ile pair that makes hydrogen bonding contacts with the carboxylate of the substrate in D-hydroxy acid DHs is colored green. A Lys residue (red) that is located in the active site of a homology model of PTDH (*9*) is conserved in the two BLAST hits with the highest level of identity, the function of which is currently unverified. It is also found in a phosphite dehydrogenase from *Alcaligenes faecalis* WM2072 (*33*). Abbreviations (% identity with PTDH, GenBank accession number): DGDH, D-glycerate DH (*Hyphomicrobium methylovorum*, 27%, P36234) (*53*); DPGDH, D-3-phosphoglycerate DH (*E. coli*, 24%, P08328) (*54*); DLDH, D-lactate DH (*Lactobacillus helveticus*, 26%, P30901) (*55*); and FDH, formate DH (*Pseudomonas* sp. 101, 25%, P33160) (*56*). GenBank accession numbers NP_478512 (*Nostoc* sp. PCC 7120, 51%) (*57*, *59*) and ZP_00110436 (*Nostoc punctiforme*, 51%). Four of these proteins, DGDH (*24*), DLDH (PDB entry 2DLD), DPGDH (*58*), and FDH (*23*), have been structurally characterized.

Scheme 1

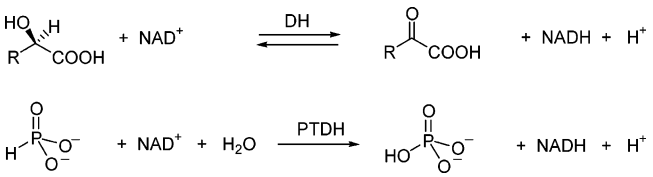

transfer step is at least partially rate-limiting as shown by kinetic isotope effects of ~2 on both k_{cat} and $k_{cat}/K_{m,phosphite}$ (*17*).

Although the D-hydroxyacid dehydrogenases have been studied in less depth and have no evolutionary relationship to the L-hydroxyacid dehydrogenases (*11*, *18*, *19*), several studies suggest a similar reaction mechanism with some distinct differences (*20*−*25*). The currently favored mechanism for the zinc-independent oxidation of D-hydroxy acids is depicted in Scheme 2. A conserved His residue (His292 PTDH numbering, Figure 1) is proposed to be the catalytic acid or base that deprotonates the alcohol during oxidation and that protonates the carbonyl during the physiologically important reduction of the substrate (*19*, *21*). In the X-ray structure of D-glycerate DH, this His residue is engaged in a short hydrogen bond (2.5 Å) with a highly conserved glutamate residue (Glu266, Figure 1) (*24*) that has been proposed to increase the pK_a of His292 and ensure its protonation at physiological pH. Similar hydrogen bond interactions between the two conserved residues are found in

Scheme 2

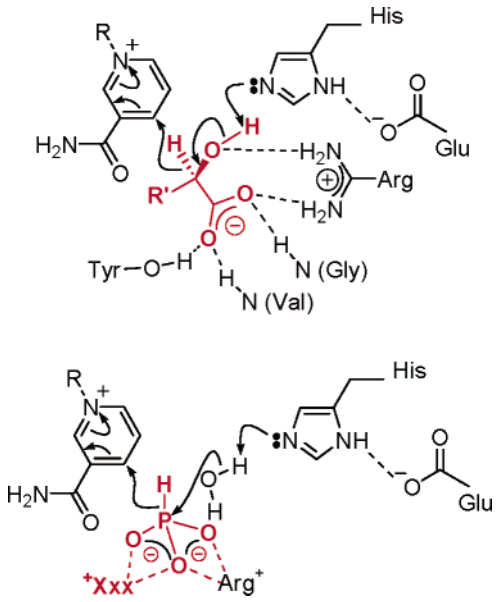

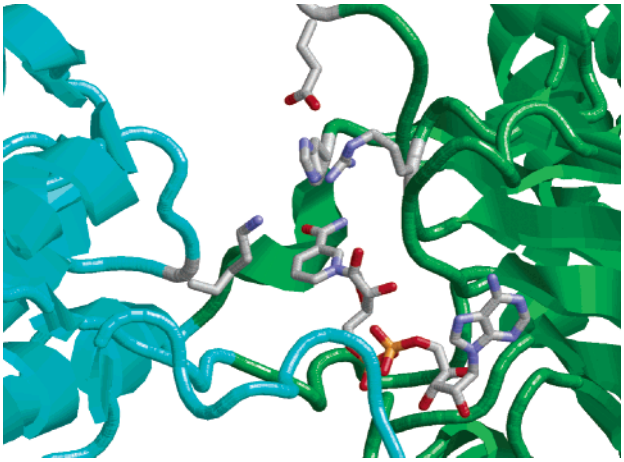

FIGURE 2: View of the active site of a homology model of phosphite dehydrogenase. The three residues that are conserved among the family of D-hydroxy DHs in the substrate-binding domain are shown in stick format (His292, Arg237, and Glu266). Also shown is the Lys residue that is conserved in putative phosphite dehydrogenases but not in other members of the D-hydroxy acid DH superfamily.

structures of other family members (*26*−*28*). In one family member, formate dehydrogenase, the Glu is replaced with a Gln, presumably because no proton transfer is required for formate oxidation. A strictly conserved Arg serves to bind the carboxylate group of the substrate (*19*, *29*). Crystallographic analyses of several D-hydroxy acid DHs suggest that this Arg also aids in polarizing the carbonyl group of the substrate for reduction by NADH (*26*−*28*, *30*). Two backbone amides from conserved Gly and Val/Ile residues make additional hydrogen bonding contacts with the carboxylate group (Scheme 2). In PTDH, this Gly is also conserved but Lys76 replaces the Val or Ile residue (Figure 1).

PTDH has a pH optimum of 7.5, which given the pK_a values of phosphorous acid, 1.5 and 6.8 (*31*, *32*), would suggest that unlike the substrate for D-hydroxy acid DHs, the active form of the substrate for PTDH is dianionic. To maintain charge neutrality in the active site, a second protonated residue besides Arg237 may therefore be involved in substrate binding. At present, no structural information is available for PTDH, but a homology model (*9*) points to Lys76 as a candidate for this residue, replacing the neutral hydrogen bond contact of the amide of the Val or Ile that occupies this position in other family members (Scheme 2 and Figure 2). This Lys residue is conserved among other known (*33*) and putative PTDHs in protein databases (>50% identity, Figure 1) but not in D-hydroxy acid DHs, consistent with a role of providing a second positive charge that is not needed for hydroxy acid binding. We report here site-directed mutagenesis studies of the three conserved active site residues, His292, Arg237, and Glu266, as well as Lys76.

MATERIALS AND METHODS

Chemicals. NAD^+ was purchased from Sigma. Phosphorous acid was purchased from Sigma-Aldrich. Deuterium-labeled phosphorous acid was prepared as described previously (*8*). Diethyl pyrocarbonate was purchased from Alfa Aesar. Ingredients for buffers and media were obtained from Fisher, Difco, or Aldrich. dNTPs were ordered from GibcoBRL and Invitrogen. Isopropyl β-D-thiogalactoside (IPTG) was ordered from CalBioChem. Dithiothreitol (DTT) was purchased from Fisher. POROS 20 MC resins used for metal chelate affinity chromatography were purchased from PerSeptive Biosystems. Centricon spin columns and Amicon membranes were obtained from Millipore. PCR purification, gel extraction, Miniprep, and Midiprep kits were provided by Qiagen. The pET15b plasmid was obtained from Novagen. Oligonucleotides for PCRs were synthesized by Integrated DNA Technologies, Inc.

Enzymes. Restriction enzymes NcoI and BamHI, *Pfx* DNA polymerase, and *Taq* polymerase were purchased from GibcoBRL. NdeI, shrimp alkaline phosphatase, and T4 DNA ligase were purchased from New England Biolabs. Thrombin was obtained from Amersham Biosciences.

Generation of Mutant Genes. An overlap extension PCR (OE-PCR) method was utilized to introduce site specific mutations into a BamHI−NcoI fragment of the PTDH gene using the purified pET11-PTDH plasmid encoding wild-type (wt) PTDH as a template (*6*). Two oligonucleotide primers flanking the fragment were used in combination with internal mutagenic primers. For the NcoI forward primer, the oligomer was complementary to the sequence approximately 50 bp upstream from the restriction site to improve restriction digestion of the PCR product and prevent a problem of multiple-site annealing encountered when the primer was located closer to the NcoI site. Flanking primer sequences follow: BamHI reverse primer, 5′ TAG CAG CCG GAT CCC CCG GGC TG 3′; NcoI forward primer, 5′ ACG GCA CGG GGC TGG ATA ACG CTA CGG 3′; Mutagenic primers follow, with underlined codons encoding desired amino acid substitutions: His292Lys forward primer, 5′ TC ACT CCG AAA ATA GGG TCG GCA GTG CGC 3′; His292Lys reverse primer, 5′ A CCC TAT TTT CGG AGT GAA CAG CGT ATT 3′; His292Asp forward primer, 5′ TC ACT CCG GAT ATA GGG TCG GCA GTG CGC 3′; His292Asp reverse primer, 5′ A CCC TAT ATC CGG AGT GAA CAG CGT ATT 3′; His292Asn forward primer, 5′ TC ACT CCG AAC ATA GGG TCG GCA GTG CGC 3′; His292Asn reverse primer, 5′ A CCC TAT GTT CGG AGT GAA CAG CGT ATT 3′; His292Phe forward primer, 5′ TC ACT CCG TTT ATA GGG TCG GCA GTG CGC 3′;

His292Phe reverse primer, 5′ GA CCC TAT AAA CGG AGT GAA CAG CGT ATT 3′; Glu266Asp forward primer, 5′ C GAA ATG GAT GAC TGG GCT CGC GCG GAC 3′; Glu266Asp reverse primer, 5′ C CCA GTC ATC CAT TTC GAA TAC ATC CGC 3′; Glu266Gln forward primer, 5′ TC GAA ATG CAA GAC TGG GCT CGC GCG GAC 3′; Glu266Gln reverse primer, 5′ GC CCA GTC TTG CAT TTC GAA TAC ATC CGC 3′; Arg237Lys forward primer, 5′ C CCC TGT AAA GGT TCG GTA GTG GAT GAA 3′; Arg237Lys reverse primer, 5′ C CGA ACC TTT ACA GGG GTT TAC AAG CAG 3′; Arg237Leu forward primer, 5′ C CCC TGT CTG GGT TCG GTA GTG GAT GAA 3′; Arg237Leu reverse primer, 5′ C CGA ACC CAG ACA GGG GTT TAC AAG CAG 3′. *Pfx* DNA polymerase was used for all PCR amplifications. Reaction mixtures contained the forward and reverse primers (each at 0.6 μM), GibcoBRL PCR buffer, dNTPs (each at 0.25 mM), 0.5−1.5 mM Mg^{2+}, 1−5 units of the polymerase, and the template DNA, in a total volume of 50 μL. PCR products were purified with the QIAquick gel extraction kit from QIAGEN.

Genes encoding the mutation of Lys76 to Ala, Arg, Cys, or Met as well as Arg237 to His or Gln were generated using mega-primer PCR. In the first PCR, the forward primer was the mutagenic primer 5′ GCT GCG CGC TCX XXG GCT TCG ACA ATT TCG 3′ for Lys76 mutations, where XXX was GCG, CGT, TGC, or ATG encoding Ala, Arg, Cys, or Met, respectively, at codon 76. For Arg237 mutations, the forward primer was 5′ GTA AAC CCC TGT XXX GGT TCG GTA GTG 3′, where XXX was CAT or GAG encoding His or Gln, respectively. The reverse primer encoded the end of the phosphite dehydrogenase gene with a flanking BamHI restriction site. The resulting gene fragment was PCR purified using the Qiagen PCR purification kit and used as a mega-primer for a second PCR with a forward primer that contained a NdeI restriction site flanking the start of the gene. The final PCR product was gel purified (Qiagen quick gel purification) digested with NdeI and BamHI and ligated into the pET15b vector as a His tag fusion. All mutant genes were sequenced with four overlapping reads to verify the mutation in the absence of other substitutions. The constructs were inserted into pET11 and pET15b vectors using the NcoI and BamHI restriction sites, or NdeI and BamHI (for Lys76 mutants and R237H,G).

Overexpression and Purification of Mutant Proteins. E. coli BL21(DE3) cells transformed with the appropriate plasmid were grown and expressed as previously described (*9*), and large-scale protein purifications of Arg237, Glu266, and His292 mutants (from 3 to 10 L cultures) were carried out as previously described (*9*). *Escherichia coli* BL21(DE3) cells harboring plasmids carrying the Lys76 mutants or the R237H/Q mutations were grown and induced on a smaller 150 mL scale. These proteins were purified using the same method used previously, but with smaller columns containing 500 μL bed volume columns of Talon immobilized metal affinity chromatography (IMAC) resin (Clontech). Correspondingly smaller wash and elution volumes of 10 and 1 mL, respectively, were used. For these smaller-scale purifications, the proteins were concentrated and re-equilibrated with 0.7 mL of buffer in Millipore Centricons with a 10 kDa molecular mass cutoff to remove the ingredients from the elution buffer. All purified proteins were stored at −80 °C in the presence of 10% glycerol and 1 mM DTT. The concentration of the protein was determined by the Bradford assay and also by measuring the absorbance at 280 nm using a theoretical extinction coefficient of 27 mM^{-1} cm^{-1}.

Removal of the Histidine Tag with Thrombin. The histidine tag of PTDH was removed by treatment of 100 μg of His_6-PTDH with 1 unit of thrombin at 16 °C for 16 h. Progression of cleavage was examined by gel electrophoresis (12% SDS−polyacrylamide, PTDH = 36.4 kDa, His_6-PTDH = 38.6 kDa). The thrombin reaction solution was transferred to a YM30 Centricon, and the protein was repeatedly concentrated by ultrafiltration followed by dilution with 50 mM MOPS buffer (pH 7.25) and reconcentration. The procedure was repeated at least 10 times to ensure that the His-tag peptide had been removed as shown by reaction of the flow through with DEPC.

Kinetic Studies. Initial rates were obtained at 25 °C using a Cary 100 Bio UV−vis spectrophotometer (Varian) with five fixed concentrations of NAD^+ and five varying concentrations of phosphite or deuterium-labeled phosphite. The concentrations of NAD^+ stock solutions were determined by UV−vis (ϵ_{NAD^+} = 18 mM^{-1} cm^{-1} at λ = 260 nm). The concentrations of phosphite stock solutions were determined by adding PTDH and excess NAD^+ (∼2 mM). The reaction mixture was incubated at 25 °C and the reaction allowed to reach completion. The concentration of phosphite in the initial solution was then determined by the concentration of NADH produced (ϵ_{NADH} = 6.22 mM^{-1} cm^{-1} at λ = 340 nm). The specific activity of the protein was determined by adding 2−75 μg of the protein to a 500 μL assay solution containing 1.0 mM NAD^+ and 1.0 mM phosphite in 50 mM MOPS (pH 7.25) at 25 °C. Assays were performed in duplicate. Values for k_{cat} and K_M were obtained by fitting the data to the equation for a sequential ordered mechanism (*34*) with NAD^+ binding first (*6*), using ENZKIN (eq 1).

$$v = \frac{V_{max}[A][B]}{K_{iA} + K_A[B] + K_B[A] + [A][B]} \quad A = NAD^+ \text{ and } B = \text{phosphite} \qquad (1)$$

pH−Rate Profiles for wt and Mutant PTDH. Solutions of 100 mM Tris, 50 mM MES, and 50 mM AcOH [a universal buffer with a constant ionic strength (*35*)] were adjusted to various pH values from 5.5 to 9.5 at 25 °C using 5 M NaOH or 5 M HCl. Stock solutions of phosphite (5−500 mM) and NAD^+ (4−20 mM) were made at each pH using the same universal buffers. A 5 × 5 matrix of various NAD^+ and phosphite concentrations was assayed at each pH, and the reaction was initiated by adding 2−6 μg of wt-PTDH or PTDH-E266Q to 500 μL of assay buffer. The pH−rate profile was obtained by plotting log *V*/*K* versus pH. pK_a values were obtained by fitting the data to eq 2 for a process involving two proton transitions (*36*).

$$\log(V/K) = \log\left[\frac{(V/K)_o}{1 + \frac{[H^+]}{K_a} + \frac{K_a'}{[H^+]}}\right] \qquad (2)$$

Stoichiometry of Histidine Alkylation. Diethyl pyrocarbonate (DEPC) solutions were freshly prepared in anhydrous acetonitrile for each experiment. The concentration of DEPC was determined by monitoring the reaction with 10 mM

imidazole (pH 7.5−8.0) at 240 nm (*37*). For all reactions, the His tag was first removed from PTDH and H292F-PTDH (see above). The time course of alkylation was followed in a cuvette by recording continuously the change in absorbance at 242 nm for 30−60 min. The number of modified histidine residues was calculated from the absorbance change at 242 nm using an ϵ of 3200 M^{-1} cm^{-1} (*38*, *39*).

Inactivation by DEPC in the Absence and Presence of Ligands. PTDH was incubated at 25 °C in 30 mM sodium phosphate buffer (pH 7.25) for 1 min in the absence of any substrates or substrate analogues, or in the presence of 1 mM NAD^+, 1 mM sulfite, or 1 mM NAD^+ with 1 mM sulfite. Aliquots of a stock solution of diethyl pyrocarbonate in acetonitrile or just acetonitrile as a control were added to the mixture to initiate the reaction resulting in final concentrations of 25−100 μM. Aliquots of 20 μL were removed at various time points from the reaction mixture and were assayed in 1 mL assay mixtures containing 1 mM NAD^+ and 1 mM phosphite in 30 mM sodium phosphate buffer (pH 7.25).

CD Spectra. WT and mutant PTDH samples were loaded onto separate Centricons (YM30 membrane) and washed thoroughly (∼10 × 1.5 mL) with 50 mM MOPS buffer (pH 7.25) to remove any adventitious reagents from the IMAC procedure. The concentrations of all samples were adjusted to an A_{280} of 0.5 and analyzed using a JASCO J-720 spectropolarimeter at the Laboratory of Fluorescence Dynamics at the University of Illinois at Urbana-Champaign (UIUC).

Cysteine Alkylation. Cys residues of wt PTDH were alkylated in the presence and absence of 1 mM NAD^+ with 40 mM 2-bromoethylamine at pH 8.5 in 100 mM Tris buffer at 25 °C for 24 h at a protein concentration of 3 mg/mL. Samples were assayed under conditions of saturating substrates to determine the effect on the wt enzyme. The Lys76Cys mutant was reacted with and without 40 mM 2-bromoethylamine at pH 8.5 in 100 mM Tris buffer at a protein concentration of 3.8 mg/mL in the presence of 2 mM NAD^+ (∼10K_m) for 17 h, at which point the controls and samples were assayed as described above.

RESULTS

Steady-State Kinetic Parameters of Mutants of His292, Arg237, and Glu266. Wild-type (wt) PTDH and all mutant proteins were heterologously expressed in *E. coli* with N-terminal His_6 tags for ease of purification by IMAC (*40*). Previous studies have shown that the recombinant tagged wt protein has only slightly reduced activity compared with the native protein (*6*, *9*). Mutation of His292 to Lys, Phe, or Asn resulted in a loss of all detectable activity when assessing production of NADH spectrophotometrically. A conservative estimate of the sensitivity of the assay (Table 1) indicates an at least 10^6-fold decrease in $k_{cat}/K_{m,phosphite}$ compared to that of wt PTDH. Replacement of Arg237 with Leu, His, and Gln similarly produced a mutant enzyme without detectable activity. However, substitution of the Arg with another basic residue (Lys) resulted in an active mutant with an ∼100-fold decrease in k_{cat}. The Michaelis constants for both phosphite and NAD^+ increased significantly with a greater effect on the former (∼120-fold vs 20-fold). Substitution of Glu266 with Gln resulted in a mutant with a surprisingly improved k_{cat} compared to that of the wt protein.

Table 1: Summary of Steady-State Kinetic Constants of wt and Mutant PTDH at pH 7.5

enzyme[a]	k_{cat} (s^{-1})	$K_{m,phosphite}$ (mM)	$k_{cat}/K_{m,phosphite}$ (M^{-1} s^{-1})	$K_{m,NAD}$ (mM)
wt	3.2 ± 0.2	0.053 ± 0.004	6.0×10^4	0.057 ± 0.007
His292Asn	−	−	$<10^{-2}$	−
His292Phe	−	−	$<10^{-2}$	−
His292Lys	−	−	$<10^{-2}$	−
Glu266Gln	8.0 ± 0.6	5.00 ± 0.06	8.0×10^3	1.0 ± 0.2
Arg237Lys	0.028 ± 0.003	6.0 ± 0.2	4.7	1.0 ± 0.1
Arg237Leu	−	−	$<10^{-2}$	−
Arg237His	−	−	$<10^{-2}$	−
Arg237Gln	−	−	$<10^{-2}$	−
Lys76Ala	0.82 ± 0.01	1.1 ± 0.2	0.75×10^3	0.26 ± 0.04
Lys76Arg	2.33 ± 0.17	0.35 ± 0.06	6.6×10^4	0.11 ± 0.01
Lys76Met	1.62 ± 0.12	2.00 ± 0.15	0.81×10^3	0.90 ± 0.06
Lys76Cys	0.58 ± 0.07	0.60 ± 0.10	0.97×10^3	0.20 ± 0.02

[a] All proteins contained an N-terminal His_6 tag.

The K_m values for both substrates do, however, increase significantly (85-fold for phosphite and ∼20-fold for NAD^+), resulting in a mutant with an overall reduced catalytic efficiency. All mutant proteins were analyzed by circular dichroism and showed no detectable differences compared to the wt protein (data not shown).

Inactivation by Diethyl Pyrocarbonate. The site-directed mutagenesis studies show that His292 is important for NAD^+ binding. To further probe the importance of this residue, wt PTDH was treated with diethyl pyrocarbonate (DEPC) after removal of the His tag. This reagent reacts selectively with accessible His residues to form *N*-carbethoxyhistidine in a pH range of 5.5−8.0 (*38*). UV−vis spectroscopic analysis of the protein at 242 nm before and after reaction revealed the presence of 6.11 ± 0.11 modified residues, in good agreement with the six His residues predicted from the homology model of PTDH to have a solvent-exposed reactive nitrogen that is not engaged in a well-defined hydrogen bond (*9*). The kinetics of modification showed multiphasic behavior with a faster phase followed by one or more slower processes (data not shown). The amplitude of the absorbance change of the fast phase suggests it results from the reaction of 2−3 His residues. Treatment with DEPC also gave rise to time-dependent loss of activity with kinetics that correlated closely with the fast phase of modification (Figure 3). To investigate whether the fast phase included reaction of His292, the His292Phe mutant was reacted with DEPC, leading to 5.5 ± 0.1 modified His residues. The amplitude of the fast phase was significantly smaller for this mutant (1−2 His), consistent with rapid modification of His292 in the wt protein. Since the His292Phe protein (and other His292 mutants) has no detectable activity, the involvement of His292 in the inactivation could not be probed directly with the mutant enzyme. The wt protein was protected from inactivation, however, by the addition of both NAD^+ and sulfite (Figure 3), a competitive inhibitor with respect to phosphite (*6*). No protection was observed in the presence of only NAD^+ or sulfite. These results provide support that the inactivation is due to modification of a His in the active site of the enzyme, which is protected in the ternary complex. Protection against inactivation by DEPC only when both NAD^+ and sulfite are present is consistent with the ordered kinetic mechanism of PTDH with NAD^+ binding first (*6*) and with the homology model that shows that His292 is still accessible after binding of just NAD^+. Unfortunately,

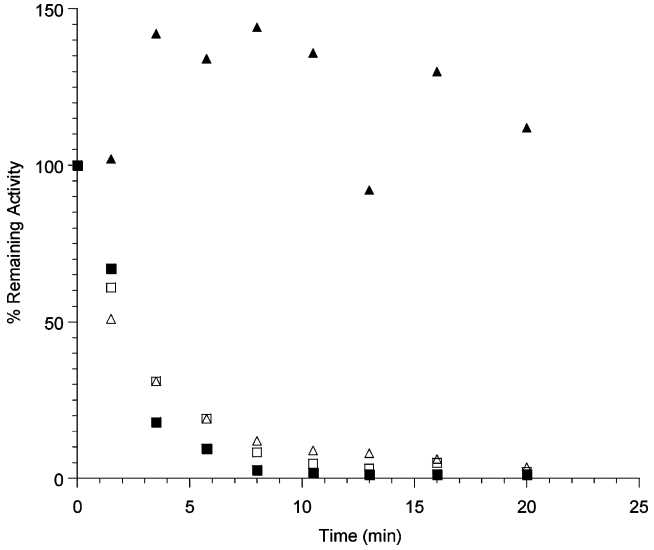

FIGURE 3: Time-dependent loss of activity after treatment of wt PTDH with 25 μM DEPC (△), with 25 μM DEPC and 1 mM NAD^+ (□), with 25 μM DEPC and 1 mM sulfite (■), and with 100 μM DEPC, 1 mM NAD^+, and 1 mM sulfite (▲).

investigation of the pH dependence of the inactivation kinetics to determine the pK_a of His292 was inconclusive, presumably due to the modification of multiple residues.

pH−Rate Profile of Glu266Gln. Wild-type PTDH displays a bell-shaped pH−rate profile for $k_{cat}/K_{m,phosphite}$ with pK_a values of 6.8 and 7.8 (*16*). Under saturated substrate conditions, k_{cat} is essentially independent of pH. On the basis of the pH dependence of the competitive inhibition by sulfite, the low-end pK_a has been attributed to the second deprotonation of the phosphite substrate (p$K_{a,2}$ = 6.8) (*16*). The high-end pK_a has been tentatively assigned to a residue that must be protonated for phosphite binding. Candidates for this residue would be the conserved Arg237 or His292 residue, or possibly Lys76. Although the pK_a of His292 could not be determined by the pH dependence of the kinetics of DEPC inactivation, it may be accessible by mutation of Glu266. In other D-hydroxy acid DHs, this Glu keeps the active site His in its protonated form by increasing its pK_a. Disruption of this interaction is expected to lower the pK_a, resulting in a shift of the basic limb of the bell curve to lower pH. The pH dependence of the Glu266Gln mutant is depicted in Figure 4. Instead of the predicted shift to a lower pH, the pK_a of the basic limb transition actually shifted slightly outward to a higher value (8.4 ± 0.2). The acidic limb of the curve corresponds to a pK_a of 7.2 ± 0.2, close to that of the wt protein. Attempts to generate the Glu266Asp mutant resulted in a mutant protein that was produced in insoluble form regardless of the conditions of the overexpression or expression system that was used.

Steady-State Kinetic Parameters of Mutants of Lys76. If not His292, two other candidate residues may govern phosphite binding with a pK_a of 7.8. One of these is Lys76, which is located in the active site cleft opposite the other three conserved residues (Figure 2). Mutation of Lys76 to Ala increased the K_m of phosphite 20-fold and that of NAD^+ 4-fold with the k_{cat} decreased by ~4-fold (Table 1). Replacement of the Lys with a Met provided a similar overall effect with the K_m values of phosphite and NAD^+ increasing 40- and 16-fold, respectively, and k_{cat} decreasing ~2-fold.

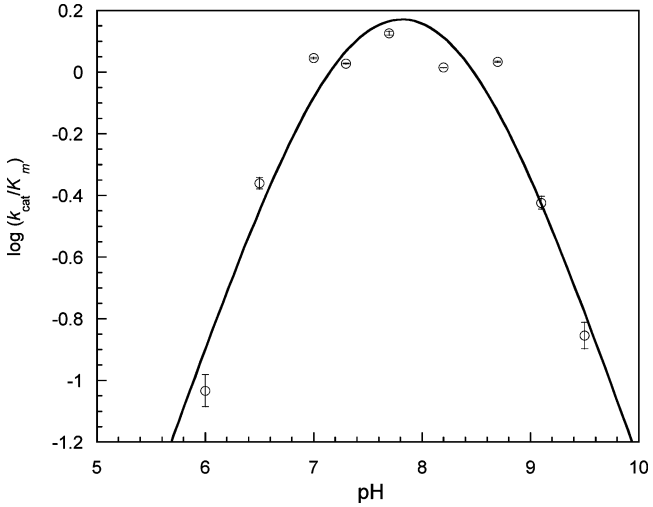

FIGURE 4: pH dependence of k_{cat}/K_m for the E266Q mutant. The line represents a nonlinear least-squares fit to eq 2.

Table 2: Summary of Steady-State Kinetic Constants of wt PTDH, the Lys76Cys Mutant, and the Lys76Cys Mutant Treated with 2-Bromoethylamine

enzyme	$K_{m,phosphite}$ (μM)	k_{cat} (s^{-1})	$k_{cat}/K_{m,phosphite}$ (M^{-1} s^{-1})
wt	53 ± 4.0	3.2 ± 0.2	6.0×10^4
Lys76Cys[a]	770 ± 130	0.43 ± 0.02	5.6×10^2
Lys76γ-thiaLys[b]	20 ± 2	0.64 ± 0.01	3.2×10^4

[a] Alkylation reaction control. [b] Cys capped with 2-bromoethylamine.

Changing the Lys to Arg resulted in much smaller changes in the steady-state kinetic parameters. To probe whether the observed data were due to local misfolding, the Lys76Cys mutant was prepared and analyzed. Its K_m values for phosphite and NAD^+ were increased by 12- and 3.5-fold, respectively, and its k_{cat} was decreased 5.5-fold compared to that of wt PTDH. The mutant enzyme was then treated with 2-bromoethylamine with the aim of alkylating the newly introduced Cys and restoring the positive charge as γ-thialysine (*41*). As a control, wt PTDH was treated with the reagent for an equal amount of time. Approximately 30% of the wt activity was lost after this treatment; however, the enzyme was completely protected from this inactivation by the addition of 1 mM NAD^+. These results are consistent with the homology model, which suggests that only one cysteine (Cys236) is located near the active site and is involved in hydrogen bonding to the 2′-hydroxyl of the nicotinamide ribose of NAD^+. Since NAD^+ protects wt PTDH from inactivation, it was included in the alkylation reaction of Lys76Cys.

Comparison of Lys76Cys PTDH treated with and without 2-bromoethylamine showed that following alkylation the K_m of the mutant for phosphite improved more than 38-fold and the catalytic efficiency (k_{cat}/K_m) was enhanced more than 60-fold and approached that of the wt enzyme (Table 2, Figure 5). Therefore, a positive charge at this position clearly enhances phosphite binding. To determine if Lys76 was responsible for the basic limb of the wt PTDH, the pH−rate profile for $k_{cat}/K_{m,phosphite}$ of Lys76Ala was determined and displayed a bell-shaped curve with a basic pK_a of 8.17 ± 0.06 (Supporting Information). The pH−rate profile of the Arg237Lys mutant, the only mutation at this position that resulted in an active enzyme, also exhibits a bell-shaped

Table 3: Substrate Kinetic Isotope Effects for wt PTDH and Two Mutants

enzyme	k_{cat}^{H}/k_{cat}^{D}	$(k_{cat}/K_{M,Pt})^{H}/(k_{cat}/K_{M,Pt})^{D}$
wt	2.1 ± 0.1	1.8 ± 0.3
Lys76Cys	2.3 ± 0.1	2.2 ± 0.2
Glu266Gln	2.1 ± 0.2	2.1 ± 0.1

curve with a pK_a value for the basic limb that has shifted to 8.4 (Supporting Information). Like that of the wild-type enzyme, k_{cat} was pH-independent for both Arg237Lys and Lys76Ala.

Primary Kinetic Isotope Effects of K76C and E266Q. Both Lys76Cys and Glu266Gln mutations resulted in perturbations of the k_{cat} and $k_{cat}/K_{m,phosphite}$ of PTDH. In the case of Glu266Gln, k_{cat} was enhanced more than 2-fold, whereas k_{cat} of Lys76Cys was reduced more than 5-fold; their $k_{cat}/K_{m,phosphite}$ values were decreased by 7- and 63-fold, respectively. The primary kinetic isotope effects (KIEs) displayed by these mutants were determined with deuterium-labeled phosphite (*17*) to probe for changes in the rate-limiting step(s) (Table 3). The k_{cat} and $k_{cat}/K_{m,phosphite}$ values for these mutants span a range greater than 1 order of magnitude, yet their kinetic isotope effects are identical within experimental error (Table 3), indicating that the degree to which the hydride transfer step is rate-limiting is maintained, and perhaps that the measured KIE is the intrinsic isotope effect, as demonstrated for formate dehydrogenase (*42*), another member of the D-hydroxy acid DH family. D-Lactate DH from *Lactobacillus pentosus* also displays only modest changes in substrate KIE on k_{cat} (1.6−2.6) for a series of active site mutants with turnover frequencies differing by 4 orders of magnitude (*20*). Whether chemistry is solely rate limiting in this case has not been determined to date.

DISCUSSION

When previous studies on D-hydroxy acid dehydrogenases are interpreted in the context of PTDH, it is important to consider the physiological role of these proteins. In general, the in vivo function of the enzymes that have D-hydroxy acids as their substrates is the *reduction* of the corresponding 2-keto acids. Hence, these proteins have evolved toward optimized K_m values for the keto acid at physiological pH. The function of formate dehydrogenase (FDH) is the *oxidation* of formate to carbon dioxide, and the role of phosphite dehydrogenase is the *oxidation* of phosphite. The latter two enzymes have not been assayed in the reverse direction because of the strong thermodynamic preference for the oxidized product ($K_{eq} = 10^{11}$ for PTDH and 5×10^3 for FDH at pH 7.0).

The role of the fully conserved His has been addressed in a number of studies on other D-hydroxy acid DHs. Substitution of the catalytic His with Tyr in D-lactate DH (DLDH) from *Lactobacillus plantarum* resulted in a protein with a greatly decreased but still measurable level of pyruvate reduction activity (*21*). On the other hand, in the direction of D-lactate oxidation, the K_m for lactate was too large to be determined. Replacement of the His with Gln further disrupted the catalytic function, and the reaction could not be saturated in either direction. These results are consistent with a proton donor being required at the position of the His residue for pyruvate binding (and reduction) and a general base for lactate binding (and oxidation). Remarkably, substitution of the His with Lys in DLDH from *Lactobacillus bulgaricus* produced an enzyme with an essentially unchanged k_{cat} and Michaelis constants for pyruvate and NAD^+ (*25, 28*). The kinetic properties of this mutant for the oxidation of D-lactate, more relevant for comparison with PTDH, have not been published. In the current study on PTDH, mutation of His292 to Asn, Lys, or Phe resulted in a protein without detectable phosphite oxidation activity (Table 1). Similar results have been reported for mutation of this residue in FDH (*43*). Collectively, these findings show that in general, the conserved His in D-hydroxy DHs is more critical for binding and oxidation of the reduced substrate than binding and reduction of the oxidized substrate.

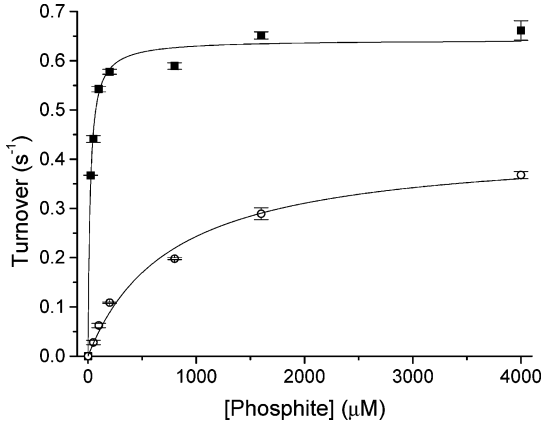

FIGURE 5: Chemical rescue of Lys76Cys PTDH. Lys76Cys PTDH was treated with 40 mM 2-bromoethylamine in 100 mM Tris (pH 8.5) and 2 mM NAD^+ (■) or with just 100 mM Tris (pH 8.5) and 2 mM NAD^+ (○). These samples were then assayed at varying concentrations of phosphite and saturating NAD^+.

In PTDH, His292 could fulfill three different roles in phosphite oxidation. In the most straightforward extrapolation of the accepted mechanism of oxidation of D-hydroxy acids (Scheme 2), it would deprotonate a water molecule for attack onto the phosphorus of phosphite. Alternatively, it could function merely as a binding residue for phosphite. And, although more speculative, it could be involved in nucleophilic catalysis, resulting in a phosphohistidine intermediate in analogy to His kinases. A phosphohistidine species is very labile, and its hydrolysis should be readily achieved with one of the other basic residues in the active site serving as a general base.

The acidic limb of the pH−rate profile with wt PTDH has been attributed to deprotonation of monoprotic phosphorous acid with the basic limb being associated with deprotonation of an enzymatic residue. Although the pK_a of His292 could not be determined directly in the DEPC inactivation studies, the effect of mutation of Glu266 to Gln could potentially be used to evaluate whether the basic limb in the pH−rate profile is linked to His292. Replacement of the corresponding Glu with Gln in D-lactate DH from *L. bulgaricus* shifts the proton transfer transition observed in the $k_{cat}/K_{m,pyruvate}$ versus pH profile by 2 units to lower pH because of the disrupted stabilization of the protonated His (*29*). A shift of the pK_a of the enzyme−NAD^+ complex in the same direction has also been reported for the Glu to Gln mutant of D-lactate DH from *L. pentosus* (*20*). Hence, these studies clearly established that in those proteins the conserved Glu serves to ensure that the His in the active site is

protonated for optimal substrate binding. However, it is clear from the pH−rate profile of the Glu266Gln PTDH mutant (Figure 4) that such a shift of the basic limb toward lower pH is not observed. Therefore, we conclude that either the protonation state of His292 does not show up in the profile for $k_{cat}/K_{m,phosphite}$ or Glu266 does not influence the pK_a of His292. Although the Glu266Gln mutation did not affect the pH−rate profile, it did increase the K_m values for both substrates and interestingly displayed an increased k_{cat}. This latter finding in conjunction with the substantial KIE that shows that chemistry is still at least partially rate-limiting rules out a role for Glu266 in stabilizing a developing positive charge on His292 in the transition state of the hydride transfer step. Most likely, the mutation disrupts the positioning of the two active site residues to which it is hydrogen bonded in the homology model, Arg237 and His292, thereby increasing the K_m of phosphite. Once the substrates are bound, the Glu residue is not important for catalysis.

The results with the Glu266Gln mutant raise the question of which residues are important in phosphite binding. It appears from the loss of activity in the Arg237Leu, Arg237His, and Arg237Gln mutants and the significant increase in the Michaelis constant for phosphite in the Arg237Lys PTDH mutant that Arg237 retains its traditional role in substrate binding and that a positive charge is essential at this position. On the other hand, Val/Ile76 that provides additional binding contacts to the carboxylate group of 2-keto acids (Scheme 2) is not conserved in PTDH. In the homology model, the backbone amide of Gly77 is still pointing into the active site cleft, but given the smaller size of phosphite compared to hydroxy acids, it is too far removed for making direct contacts with the substrate. Instead, the side chain of the Lys that replaces the Val or Ile residue (Lys76, Figure 1) is situated well for interaction with phosphite (Figure 2). The effect of the Lys mutants on the K_m for phosphite (Table 1) is much greater than on the other kinetic parameters, consistent with a role of this residue in phosphite binding. The almost complete rescue of catalytic efficiency after alkylation of the Lys76Cys mutant with 2-bromoethylamine also supports its role in phosphite binding. However, unlike the results with mutants of Arg237, a positive charge is not absolutely required at residue 76. Furthermore, the pH dependence of the k_{cat}/K_m−rate profile for the Lys76Ala mutant is essentially unaltered, ruling out the possibility that the residue with a pK_a of 7.8 is Lys76. This leaves Arg237 as a possible candidate for this residue. Unfortunately, mutation of Arg237 to nonbasic residues abolishes phosphite oxidation activity, and mutation to Lys does not significantly change the observed pK_a (8.4) for the basic limb of the pH−rate profile. Hence, Arg237 cannot be ruled out as the residue responsible for this proton transition. One other possibility exists, however, if the enzyme utilizes a reverse protonation mechanism as described below. Such mechanisms have been uncovered for several enzymes in recent years (*36*, *44*−*49*).

In the most straightforward interpretation of the pH−rate profile, the substrate must be deprotonated and a residue on PTDH must be protonated for maximal activity (Figure 6, left side). In a reverse protonation mechanism, the substrate and enzyme protonation states that lead to a productive collision complex would consist of monoprotonated phosphite and a deprotonated active site residue (Figure 6, right side). When the microscopic pK_a values are separated by less than 2 units, the pH−rate profiles for a reaction that follows either the normally protonated or the reverse protonated mechanism will both be bell-shaped with very similar macroscopic group pK_a values (*34*) (for a good graphic presentation of an example, see ref *49*). In the case of PTDH, such a reverse protonation mechanism could explain the relatively low catalytic efficiency despite the high thermodynamic driving force since only a very small fraction of enzyme and substrate would be in the correct protonation state at the optimal pH.

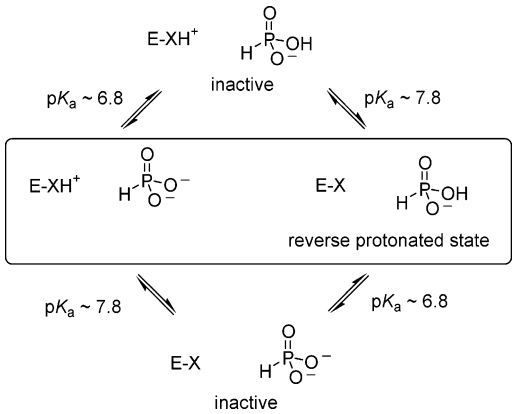

FIGURE 6: Possible protonation states of the phosphite substrate and PTDH with the potential active forms inside the box. In a mechanism that utilizes a regular protonation state (left side), the dianionic form of phosphorous acid is the true substrate and an enzymatic residue must be protonated for binding. In a reverse protonation mechanism, the group with the lower pK_a, here phosphite monoanion, will be protonated whereas the group with the higher pK_a, here a residue on PTDH, will be deprotonated in the active enzyme−substrate collision complex.

If operational, why would PTDH utilize a reverse protonation mechanism? The answer may lie in the origin of the enzyme. Phosphite has yet to be reported as a natural constituent of the environment, but it has been used in past decades in industrial settings. It is therefore conceivable that phosphite oxidation is a relatively recent activity that has not yet been fully optimized, which is supported by its low catalytic efficiency. Because its original substrate was monoanionic, the use of monoanionic phosphite by PTDH could be a remnant of its ancestral activity. Furthermore, whereas use of the monoprotonated form may constitute a thermodynamic disadvantage, it is possible that this is offset by a kinetic advantage of using the monoanionic substrate in the hydride transfer step. NMR spectroscopic studies are ongoing in an attempt to support or refute the hypothesis that phosphite binds to PTDH in its monoanionic form and to determine the pK_a of His292.

In summary, the mutagenesis and other studies presented here support roles of substrate binding for Arg237 and Lys76. The latter residue represents a useful marker for annotating genes encoding members of the D-hydroxy acid DH family as phosphite dehydrogenases. Mutation of His292 results in abolishment of phosphite oxidation, indicating its essential role in phosphite oxidation. The most likely role for His292 is activation of a nucleophile for phosphite oxidation. Whether that nucleophile is water or whether His292 itself could be the nucleophile cannot be concluded from the available data. Unfortunately, thiophosphite is not a substrate for PTDH (*16*), precluding distinction between these two possibilities through stereochemical studies (i.e., inversion

vs retention) assuming that hydride displacement occurs by an in-line displacement and does not involve metaphosphate as an intermediate (*16*, *50*). Glu266 is not essential, ruling out a role as an active site nucleophile in covalent catalysis. It is important for phosphite binding but only through positioning of other active site residues. It does not appear to control the protonation state of His292 as in other family members. The pH−rate profile of the enzyme in combination with the mutagenesis studies suggests that a reverse protonation mechanism is a possibility for PTDH, which needs to be corroborated by future spectroscopic studies.

ACKNOWLEDGMENT

The CD experiments were performed at the Laboratory for Fluorescence Dynamics (LFD) at UIUC. The LFD is supported jointly by the National Center for Research Resources of the National Institutes of Health (PHS 5 P41-RRO3155) and UIUC.

SUPPORTING INFORMATION AVAILABLE

Coordinates of the homology model of the enzyme in PDB format and pH−rate profiles for Lys76Ala and Arg237Lys. This material is available free of charge via the Internet at http://pubs.acs.org.

REFERENCES

1. Seidel, H. M., Freeman, S., Seto, H., and Knowles, J. R. (1988) Phosphonate Biosynthesis: Isolation of the Enzyme Responsible for the Formation of a Carbon−Phosphorus Bond, *Nature 335*, 457−458.
2. Kim, J., and Dunaway-Mariano, D. (1996) Phosphoenolpyruvate mutase catalysis of phosphoryl transfer in phosphoenolpyruvate: Kinetics and mechanism of phosphorus−carbon bond formation, *Biochemistry 35*, 4628−4635.
3. McGrath, J. W., Wisdom, G. B., McMullan, G., Larkin, M. J., and Quinn, J. P. (1995) The purification and properties of phosphonoacetate hydrolase, a novel carbon−phosphorus bond-cleavage enzyme from *Pseudomonas fluorescens* 23F, *Eur. J. Biochem. 234*, 225−230.
4. Olsen, D. B., Hepburn, T. W., Moos, M., Mariano, P. S., and Dunaway-Mariano, D. (1988) Investigation of the *Bacillus cereus* phosphonoacetaldehyde hydrolase. Evidence for a Schiff base mechanism and sequence analysis of an active-site peptide containing the catalytic lysine residue, *Biochemistry 27*, 2229−2234.
5. Baker, A. S., Ciocci, M. J., Metcalf, W. W., Kim, J., Babbitt, P. C., Wanner, B. L., Martin, B. M., and Dunaway-Mariano, D. (1998) Insights into the mechanism of catalysis by the P−C bond-cleaving enzyme phosphonoacetaldehyde hydrolase derived from gene sequence analysis and mutagenesis, *Biochemistry 37*, 9305−9315.
6. Costas, A. M., White, A. K., and Metcalf, W. W. (2001) Purification and characterization of a novel phosphorus-oxidizing enzyme from *Pseudomonas stutzeri* WM88, *J. Biol. Chem. 276*, 17429−17436.
7. White, A. K., and Metcalf, W. W. (2002) Isolation and biochemical characterization of hypophosphite/2-oxoglutarate dioxygenase. A novel phosphorus-oxidizing enzyme from *Pseudomonas stutzeri* WM88, *J. Biol. Chem. 277*, 38262−38271.
8. Vrtis, J. M., White, A., Metcalf, W. W., and van der Donk, W. A. (2002) Phosphite Dehydrogenase, a New Versatile Cofactor Regeneration Enzyme, *Angew. Chem., Int. Ed. 41*, 3257−3259.
9. Woodyer, R., van der Donk, W. A., and Zhao, H. (2003) Relaxing the Nicotinamide Cofactor Specificity of Phosphite Dehydrogenase by Rational Design, *Biochemistry 42*, 11604−11614.
10. van der Donk, W. A., and Zhao, H. (2003) Recent developments in pyridine nucleotide regeneration, *Curr. Opin. Biotechnol. 14*, 421−426.
11. Grant, G. A. (1989) A new family of 2-hydroxyacid dehydrogenases, *Biochem. Biophys. Res. Commun. 165*, 1371−1374.
12. Banner, M. R., and Rosalki, S. B. (1967) Glyoxylate as a substrate for lactate dehydrogenase, *Nature 213*, 726−727.
13. Warren, W. A. (1970) Catalysis of both oxidation and reduction of glyoxylate by pig heart lactate dehydrogenase isozyme 1, *J. Biol. Chem. 245*, 1675−1681.
14. Lluis, C., and Bozal, J. (1977) Kinetic formulations for the oxidation and the reduction of glyoxylate by lactate dehydrogenase, *Biochim. Biophys. Acta 480*, 333−342.
15. Duncan, R. J., and Tipton, K. F. (1969) The oxidation and reduction of glyoxylate by lactic dehydrogenase, *Eur. J. Biochem. 11*, 58−61.
16. Relyea, H. A., Vrtis, J. M., Woodyer, R., Rimkus, S. A., and van der Donk, W. A. (2005) Inhibition and pH Dependence of Phosphite Dehydrogenase, *Biochemistry* (submitted for publication).
17. Vrtis, J. M., White, A., Metcalf, W. W., and van der Donk, W. A. (2001) Phosphite Dehydrogenase: An unusual Phosphoryl Transfer Reaction, *J. Am. Chem. Soc. 123*, 2672−2673.
18. Kochhar, S., Hunziker, P. E., Leong-Morgenthaler, P., and Hottinger, H. (1992) Evolutionary relationship of NAD^+-dependent D-lactate dehydrogenase: Comparison of primary structure of 2-hydroxy acid dehydrogenases, *Biochem. Biophys. Res. Commun. 184*, 60−66.
19. Taguchi, H., and Ohta, T. (1991) D-Lactate dehydrogenase is a member of the D-isomer-specific 2-hydroxyacid dehydrogenase family. Cloning, sequencing, and expression in *Escherichia coli* of the D-lactate dehydrogenase gene of *Lactobacillus plantarum*, *J. Biol. Chem. 266*, 12588−12594.
20. Taguchi, H., Ohta, T., and Matsuzawa, H. (1997) Involvement of Glu-264 and Arg-235 in the essential interaction between the catalytic imidazole and substrate for the D-lactate dehydrogenase catalysis, *J. Biochem. 122*, 802−809.
21. Taguchi, H., and Ohta, T. (1993) Histidine 296 is essential for the catalysis in *Lactobacillus plantarum* D-lactate dehydrogenase, *J. Biol. Chem. 268*, 18030−18034.
22. Taguchi, H., and Ohta, T. (1994) Essential role of arginine 235 in the substrate-binding of *Lactobacillus plantarum* D-lactate dehydrogenase, *J. Biochem. 115*, 930−936.
23. Lamzin, V. S., Dauter, Z., Popov, V. O., Harutyunyan, E. H., and Wilson, K. S. (1994) High-resolution structures of holo and apo formate dehydrogenase, *J. Mol. Biol. 236*, 759−785.
24. Goldberg, J. D., Yoshida, T., and Brick, P. (1994) Crystal structure of a NAD-dependent D-glycerate dehydrogenase at 2.4 Å resolution, *J. Mol. Biol. 236*, 1123−1140.
25. Kochhar, S., Lamzin, V. S., Razeto, A., Delley, M., Hottinger, H., and Germond, J. E. (2000) Roles of His205, His296, His303 and Asp259 in catalysis by NAD^+-specific D-lactate dehydrogenase, *Eur. J. Biochem. 267*, 1633−1639.
26. Stoll, V. S., Kimber, M. S., and Pai, E. F. (1996) Insights into substrate binding by D-2-ketoacid dehydrogenases from the structure of *Lactobacillus pentosus* D-lactate dehydrogenase, *Structure 4*, 437−447.
27. Dengler, U., Niefind, K., Kiess, M., and Schomburg, D. (1997) Crystal structure of a ternary complex of D-2-hydroxyisocaproate dehydrogenase from *Lactobacillus casei*, NAD^+ and 2-oxoisocaproate at 1.9 Å resolution, *J. Mol. Biol. 267*, 640−660.
28. Razeto, A., Kochhar, S., Hottinger, H., Dauter, M., Wilson, K. S., and Lamzin, V. S. (2002) Domain closure, substrate specificity and catalysis of D-lactate dehydrogenase from *Lactobacillus bulgaricus*, *J. Mol. Biol. 318*, 109−119.
29. Kochhar, S., Chuard, N., and Hottinger, H. (1992) Glutamate 264 modulates the pH dependence of the NAD^+-dependent D-lactate dehydrogenase, *J. Biol. Chem. 267*, 20298−20301.
30. Vinals, C., De Bolle, X., Depiereux, E., and Feytmans, E. (1995) Knowledge-based modeling of the D-lactate dehydrogenase three-dimensional structure, *Proteins 21*, 307−318.
31. Smith, R. M., and Martell, A. E. (1976) *Critical Stability Constants*, Vol. 4, Plenum Press, New York.
32. Hess, K., Philippoff, W., and Kiessig, H. (1939) Viscosity determinations, density measurements and X-ray investigations of soap solutions, *Kolloid Z. 88*, 40−51.
33. Wilson, M. M., and Metcalf, W. W. (2005) Genetic diversity and horizontal transfer of genes involved in the oxidation of reduced P compounds by *Alcaligenes faecalis* WM2072, *Appl. Environ. Microbiol.* (in press).
34. Cleland, W. W. (1977) Determining the chemical mechanisms of enzyme-catalyzed reactions by kinetic studies, *Adv. Enzymol. 45*, 273−387.

35. Ellis, K. J., and Morrison, J. F. (1982) Buffers of constant ionic strength for studying pH-dependent processes, *Methods Enzymol. 87*, 405−426.
36. Cleland, W. W. (1982) The use of pH studies to determine chemical mechanisms of enzyme-catalyzed reactions, *Methods Enzymol. 87*, 390−405.
37. Dickenson, C. J., and Dickinson, F. M. (1975) The role of an essential histidine residue of yeast alcohol dehydrogenase, *Eur. J. Biochem. 52*, 595−603.
38. Miles, E. W. (1977) Modification of histidyl residues in proteins by diethylpyrocarbonate, *Methods Enzymol. 47*, 431−442.
39. Hennecke, M., and Plapp, B. V. (1983) Involvement of histidine residues in the activity of horse liver alcohol dehydrogenase, *Biochemistry 22*, 3721−3728.
40. Porath, J. (1992) Immobilized metal ion affinity chromatography, *Protein Expression Purif. 3*, 263−281.
41. Smith, H. B., and Hartman, F. C. (1988) Restoration of activity to catalytically deficient mutants of ribulosebisphosphate carboxylase/oxygenase by aminoethylation, *J. Biol. Chem. 263*, 4921−4925.
42. Blanchard, J. S., and Cleland, W. W. (1980) Kinetic and chemical mechanisms of yeast formate dehydrogenase, *Biochemistry 19*, 3543−3550.
43. Tishkov, V. I., Matorin, A. D., Rojkova, A. M., Fedorchuk, V. V., Savitsky, P. A., Dementieva, L. A., Lamzin, V. S., Mezentzev, A. V., and Popov, V. O. (1996) Site-directed mutagenesis of the formate dehydrogenase active centre: Role of the His332-Gln313 pair in enzyme catalysis, *FEBS Lett. 390*, 104−108.
44. Mock, W. L., and Stanford, D. J. (1996) Arazoformyl dipeptide substrates for thermolysin. Confirmation of a reverse protonation catalytic mechanism, *Biochemistry 35*, 7369−7377.
45. Price, N. E., and Cook, P. F. (1996) Kinetic and chemical mechanisms of the sheep liver 6-phosphogluconate dehydrogenase, *Arch. Biochem. Biophys. 336*, 215−223.
46. Mock, W. L., and Cheng, H. (2000) Principles of hydroxamate inhibition of metalloproteases: Carboxypeptidase A, *Biochemistry 39*, 13945−13952.
47. Naught, L. E., and Tipton, P. A. (2001) Kinetic mechanism and pH dependence of the kinetic parameters of *Pseudomonas aeruginosa* phosphomannomutase/phosphoglucomutase, *Arch. Biochem. Biophys. 396*, 111−118.
48. Vocadlo, D. J., Wicki, J., Rupitz, K., and Withers, S. G. (2002) A case for reverse protonation: Identification of Glu160 as an acid/base catalyst in *Thermoanaerobacterium saccharolyticum* β-xylosidase and detailed kinetic analysis of a site-directed mutant, *Biochemistry 41*, 9736−9746.
49. Sims, P. A., Larsen, T. M., Poyner, R. R., Cleland, W. W., and Reed, G. H. (2003) Reverse protonation is the key to general acid−base catalysis in enolase, *Biochemistry 42*, 8298−8306.
50. Relyea, H., and van der Donk, W. A. (2005) Mechanism and Applications of Phosphite Dehydrogenase, *Bioorg. Chem.* (in press).
51. Wierenga, R. K., De Maeyer, M. C. H., and Hol, W. G. J. (1985) Interaction of Pyrophosphate Moieties with α-Helixes in Dinucleotide Binding Proteins, *Biochemistry 24*, 1346−1357.
52. Rossmann, M. G., Moras, D., and Olsen, K. W. (1974) Chemical and biological evolution of nucleotide-binding protein, *Nature 250*, 194−199.
53. Yoshida, T., Yamaguchi, K., Hagishita, T., Mitsunaga, T., Miyata, A., Tanabe, T., Toh, H., Ohshiro, T., Shimao, M., and Izumi, Y. (1994) Cloning and expression of the gene for hydroxypyruvate reductase (D-glycerate dehydrogenase) from an obligate methylotroph *Hyphomicrobium methylovorum* GM2, *Eur. J. Biochem. 223*, 727−732.
54. Tobey, K. L., and Grant, G. A. (1986) The nucleotide sequence of the serA gene of *Escherichia coli* and the amino acid sequence of the encoded protein, D-3-phosphoglycerate dehydrogenase, *J. Biol. Chem. 261*, 12179−12183.
55. Bernard, N., Ferain, T., Garmyn, D., Hols, P., and Delcour, J. (1991) Cloning of the D-lactate dehydrogenase gene from *Lactobacillus delbrueckii* subsp. *bulgaricus* by complementation in *Escherichia coli*, *FEBS Lett. 290*, 61−64.
56. Popov, V. O., Shumilin, I. A., Ustinnikova, T. B., Lamzin, V. S., and Egorov, Ts. A. (1990) NAD-dependent formate dehydrogenase from methylotrophic bacteria *Pseudomonas* sp. 101. I. Amino acid sequence, *Bioorg. Khim. 16*, 324−335.
57. Kaneko, T., Nakamura, Y., Wolk, C. P., Kuritz, T., Sasamoto, S., Watanabe, A., Iriguchi, M., Ishikawa, A., Kawashima, K., Kimura, T., Kishida, Y., Kohara, M., Matsumoto, M., Matsuno, A., Muraki, A., Nakazaki, N., Shimpo, S., Sugimoto, M., Takazawa, M., Yamada, M., Yasuda, M., and Tabata, S. (2001) Complete genomic sequence of the filamentous nitrogen-fixing cyanobacterium *Anabaena* sp. strain PCC 7120, *DNA Res. 8*, 205−213.
58. Schuller, D. J., Grant, G. A., and Banaszak, L. J. (1995) The allosteric ligand site in the Vmax-type cooperative enzyme phosphoglycerate dehydrogenase, *Nat. Struct. Biol. 2*, 69−76.
59. Kaneko, T., Nakamura, Y., Wolk, C. P., Kuritz, T., Sasamoto, S., Watanabe, A., Iriguchi, M., Ishikawa, A., Kawashima, K., Kimura, T., Kishida, Y., Kohara, M., Matsumoto, M., Matsuno, A., Muraki, A., Nakazaki, N., Shimpo, S., Sugimoto, M., Takazawa, M., Yamada, M., Yasuda, M., and Tabata, S. (2001) Complete genomic sequence of the filamentous nitrogen-fixing cyanobacterium *Anabaena* sp. strain PCC 7120, *DNA Res. 8*, 227−253.

BI047868C